FEATURE ARTICLE

Functional Metalloproteins Integrated with Conductive Substrates: Detecting Single Molecules and Sensing Individual Recognition Events

B. Bonanni,[†,‡] L. Andolfi,[†] A. R. Bizzarri,[†] and S. Cannistraro*[,†]

Biophysics and Nanoscience Centre, CNISM, and CNR-INFM Facoltà di Scienze, Università della Tuscia, Largo dell'Università, I-01100 Viterbo, Italy

Received: January 3, 2007; In Final Form: February 28, 2007

In the past decade, there has been significant interest in the integration of biomaterials with electronic elements: combining biological functions of biomolecules with nanotechnology offers new perspectives for implementation of ultrasensitive hybrid nanodevices. In particular, great attention has been devoted to redox metalloproteins, since they possess unique characteristics, such as electron-transfer capability, possibility of gating redox activity, and nanometric size, which make them appealing for bioelectronics applications at the nanoscale. The reliable connection of redox proteins to electrodes, aimed at ensuring good electrical contact with the conducting substrate besides preserving protein functionality, is a fundamental step for designing a hybrid nanodevice and calls for a full characterization of the immobilized proteins, possibly at the single-molecule level. Here, we describe how a multitechnique approach, based on several scanning probe microscopy techniques, may provide a comprehensive characterization of different metalloproteins on metal electrodes, disclosing unique information not only about morphological properties of the adsorbed molecules but also about the effectiveness of electrical coupling with the conductive substrate, or even concerning the preserved biorecognition capability upon adsorption. We also show how the success of an immobilization strategy, which is of primary importance for optimal integration of metalloproteins with a metal electrode, can be promptly assessed by means of the proposed approach. Besides the characterization aspect, the complementary employment of the proposed techniques deserves major potentialities for ultrasensitive detection of adsorbed biomolecules. In particular, it is shown how sensing of single metalloproteins may be optimized by monitoring the most appropriate observable. Additionally, we suggest how the combination of several experimental techniques might offer increased versatility, real-time response, and wide applicability as a detection method, once a reproducible correlation among signals coming from different single-molecule techniques is established.

I. Introduction

Recent years have witnessed significant interest in bioelectronics, a rapidly growing research field at the junction of biochemistry, physics, biology, and nanotechnology, which is based on the integration of biomaterials with electronic elements.[1−4] Indeed, integrating biological building blocks of life, for example, proteins and nucleic acids, into synthetic materials and devices allows combining natural biological functions (such as self-assembly, catalysis, biorecognition) with the processing power of modern microelectronics with important applications in several areas, such as biodiagnostics, health care, drug screening, and environmental monitoring.[5,6]

In this context, considerable effort is being devoted to the development of ultrasensitive, fast, and reliable nano-biosensors to be employed in environmental or medical early diagnostics. Biosensors are commonly based on biomolecules coupled to microelectronic or optical transducers and on a variety of surface-based detection principles. The detection relies on biorecognition between the reagent biomolecules and sample molecules: when the biomolecules selectively react with the molecules they are designed to sense, a detectable signal is obtained from the sensor. Most modern biosensors are nowadays capable of detecting very low amounts of various biological species (in the range of 10^{-15} M);[7,8] nevertheless, these concentrations often correspond to a situation in which a medical disease, or also an environmental pollution, is significantly advanced.

Nanotechnology provides new tools to further decrease the detection limit, for instance, by integrating a single biomolecule with nanostructured materials,[5,9−11] so that nowadays important advances are taking place in nanomaterial-based biodiagnostic assays.[8] As a matter of fact, a target binding event involving a nanomaterial can have a significant effect on its physical and chemical properties, which is not necessarily found in a bulk structure made of the same material (this is the case, for instance, of nanowire[12] or carbon nanotube[13] conductive response, or also the Raman cross section for molecules adsorbed on metal

* Corresponding author. E-mail: cannistr@unitus.it. Present address: Biophysics and Nanoscience Centre, CNISM Facoltà di Scienze, Università della Tuscia, Largo dell'Università, I-01100 Viterbo, Italy. Phone: +39 0761 357136. Fax: +39 0761 357136. Home page: http://www.unitus.it/biophysics/.

† Biophysics and Nanoscience Centre, CNISM.

‡ CNR-INFM Facoltà di Scienze.

10.1021/jp070035m CCC: $37.00
Published on Web 04/11/2007

Beatrice Bonanni graduated in Physics at the University of Rome (Italy) "La Sapienza" where in 1996 she received her Ph.D. degree in Materials Science. After a 5-year postdoctoral fellowship at the Advanced Technology and nanoSCience (TASC) Laboratory in Trieste, where she focused her research on wide-gap semiconductor nanostructures for applications in optoelectronics, in 2001, she joined the Biophysics & Nanoscience Centre in Viterbo as a researcher. Since then, she extended her research to the investigation of biomaterials integrated with conductive substrates at the nanoscale, with particular interest in the preserved biorecognition capability of adsorbed macromolecules for nano-biosensing applications. She is currently at the Physics Department of University of Rome "Tor Vergata".

Laura Andolfi received her degree in Biology in 1997 from the University of Tuscia Viterbo. In 2004, she obtained her Ph.D. from the Leiden University (The Netherlands). Currently, she is a Fellow Researcher at the Faculty of Science at the University of Tuscia Viterbo supported by the "Brain Gain Project" granted by the Italian Ministry of Research and University (MUR). Her research interests include genetic engineering, application of nanoscopies to the study of morphology, and conductive properties of single biomolecules integrated with metallic electrodes.

Anna Rita Bizzarri received her degree in Physics in 1987 from the University of Rome "La Sapienza". She obtained a Ph.D. in Biophysics in 1992 from the International School of Advanced Studies (SISSA) in Trieste. After postdoctoral fellowships in Perugia (Italy) and Mainz (Germany), in 1995, she joined the Faculty of Science of the University of Tuscia in Viterbo (Italy), as Researcher. In 2000, she became Associate Professor of Physics and Laboratory of Physics. In 2006, she got the position of full Professor. Her scientific interests include spectroscopic investigations of metalloproteins, and in particular of electron-transfer proteins, even with the support of molecular dynamics simulations. At present, her interest is focused on single-molecule detection by surface-enhanced raman spectroscopy and scanning probe microscopy (SPM) approaches for both fundamental and applicative research.

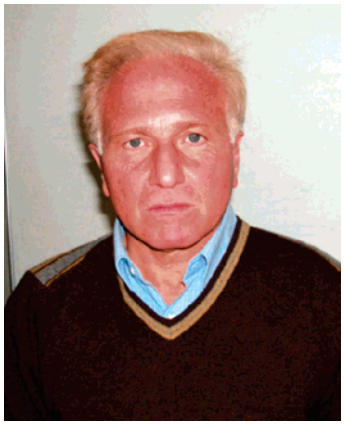

Salvatore Cannistraro obtained his degree in Physics in 1972 from the University of Pisa (Italy). He graduated in Biophysics in 1975 at the University of Liège (Belgium). After a postdoctoral fellowship in Italian National Institute of Health, he became Reader of Biophysics at the University of Calabria (Italy). He moved to the University of Perugia in 1981 as Associate Professor of Molecular Physics. Since 1992, he has been Professor of Physics, Biophysics and Nanoscience at the University of Tuscia in Viterbo where he leads the Biophysics & Nanoscience Centre. His scientific interests regard optical, magnetic, neutron spectroscopy, and molecular dynamics simulation of amorphous and biological systems. More recently, he has focused his scientific activity on the application of AFM, STM, and Raman SERS to single biomolecule detection, nano-biotechnology, and nanomedicine.

nanoparticles[8]). The improved detection limit of these systems is also a result of the enhanced signal-to-noise ratio which can be achieved at the nanoscale, together with the possibility to monitor single-electron conduction.[8] The combination of biomaterials at the nanoscale with several sensing methods (optical, electrical, electrochemical, magnetic) has to be deeply explored with the aim to pave the way to new modalities of early diagnostics.[8] In this respect, gold surfaces have emerged as attractive solid supports for the realization of hybrid systems for bioelectronic applications, owing to the chance to enable both optical and electrical transduction schemes[7,14] and for the ability to stably bind various kinds of biomolecules in a controlled way (from monolayer coverage down to single molecule) without impairing their biological activity.[15−21]

Besides the applicative aspects, the recent advances in nanotechnology also present a significant return for fundamental studies, allowing investigation of biomaterials at the nanoscale both in their natural environment and as part of hybrid systems; considering that most biological reactions occur at surfaces and interfaces, exploring mutual interaction between individual biomolecules and various surfaces allows addressing outstanding questions belonging to biology, chemistry, and physical science.[22−24]

Noticeably, these fundamental studies are, at the same time, of primary importance also for the applicative aspects: the final quality of a hybrid device passes through a comprehensive study of the biomolecules coupled to the nonbiotic elements, in terms of topology, spectroscopy, and conductive properties, possibly

at the single-molecule level. In particular, the optimal design and implementation of a nano-biosensor, with maximized sensitivity and reliability, requires that the biorecognition capability of the single biomolecule is ascertained and possibly optimized and that a good communication between the individual macromolecule and the transducer is established.

Hybrid devices which employ metalloproteins as the bioactive interface represent one of the most extensively investigated assemblies.[1,3,25−29] The possible integration of these proteins with electronic transducers has been recently explored with the aim to "wire them up" in efficient electron-transfer (ET) chains for biosensing applications at the level of the single molecule.[15,25] Indeed, these proteins have an inherent ET capability (thanks to the presence of a redox center), which is very efficient, with the ET process occurring over long distances and in a very fast, directional way.[30] Moreover, metalloproteins are, in general, part of ET chains where the conduction through the biomolecule occurs at the level of the single electron.[31,32] These characteristics, besides the nanoscale dimensions and possibility of gating redox activity, made metalloproteins a good candidate for incorporation in hybrid submicrometer-sized electronic components.[25−28] Noticeably, the preserved biorecognition capability of a single adsorbed redox protein which is also electrically coupled with a conductive substrate might offer advanced detection modes of individual recognition events (e.g., by revealing very small variations in the conductive response) and therefore need to be deeply explored.

In general, the adsorption of biomolecules, as also metalloproteins, on a surface may take advantage of self-assembling fabrication techniques,[33,34] which allow the arrangement of molecules, or groups of molecules, in arrays by simply dipping the substrate in a suitable solution, thus representing a simple alternative to conventional optical lithographic techniques. A variety of strategies have been followed to join metalloproteins and electronic components, also intended to preserve molecule functionality besides achieving an efficient electronic connection with the substrate.

Above all, chemisorption, ensuring a direct and specific linking of the biomolecule with the conductive substrate, provides immobilization of the protein with preferential orientation, also favoring the electronic connection with the substrate. In the case of gold electrodes, thiols of cysteine residues naturally available[35−39] or genetically engineered[40,41] have often been exploited: thanks to the high affinity of the thiol group for gold,[42−44] the proteins are directly linked to the substrate via S−Au bonds. However, in some cases, the strong interaction of the protein with the metallic surface can result in a loss of electrical signal[45−47] and partial protein denaturation.[1,37,48−50] In order to shelter the molecule from possible destructive interactions with the metal, a spacer of suitable length can be introduced. For instance, thiol-terminated chains can be easily deposited on Au surfaces,[42,43] forming self-assembled monolayers (SAMs); the reactive function at the other end of the spacer can be suitably chosen for specific interaction with one group of the protein. As a result, the protein is confined at a defined distance from the surface with a preferential orientation, possibly suited for fast electron exchange;[34,51−54] additionally, the linkage through chemical bonds, between the spacer and both the protein and conductive substrate, is expected to optimize the conduction through the molecule toward the electrode, thus resulting in being optimal also for possible applications of the hybrid system in nano-bioelectronics.

Paying attention to the issues discussed here, we present a comprehensive study about integration of different redox proteins with conductive substrates. We focus on testing the success of the immobilization strategy (a crucial step in designing a hybrid nanodevice) which is intended to preserve biomolecule functionality and ensure good coupling with the electrode, and we propose a number of alternatives for the detection and characterization of individual adsorbed metalloproteins. To this aim, we report results obtained with different techniques (nanoscopic and spectroscopic) which are capable of single-molecule resolution: the multitechnique approach, besides providing a widespread characterization of the adsorbed molecules, also allows detection of adsorbed biomolecules by means of recording the most appropriate among different types of signals (for instance, topography, conduction, ET, or even biorecognition capability). The combination of different experimental approaches also deserves major potentialities for novel ultrasensitive biodetection methods, since if a reproducible correspondence between signals coming from different single-molecule techniques is established, just one of the signals can be used as readout, with great advantages in sensitivity, rapidity, and efficacy of the detection.

II. Protein Assembly on a Gold Electrode

II.A. Preparation Methodologies. The direct site-specific attachment of redox proteins to gold has been investigated following two approaches, namely, focusing both on wild-type metalloproteins, which can be directly chemisorbed onto gold electrodes via exposed cysteine residues, and on engineered biomolecules, suitably mutated to introduce an anchoring group. For instance, wild-type azurin (AZ) and yeast cytochrome *c* (YCC), bearing a disulfide bridge and a free cysteine residue, respectively, can be covalently immobilized on a bare gold surface.[35,36] Of course, in this case, the (preferential) orientation cannot be decided a priori, since it is determined by the position of the anchoring group in the wild-type protein; therefore, a check that the anchoring group is not in the region involved, for instance, in biorecognition is desirable. Conversely for other metalloproteins, such as plastocyanin (PC), direct linking with gold can be attained thanks to a disulfide bridge (or also a thiol) introduced in a well-defined site of the molecule by means of genetic mutation.[55] The latter approach allows selecting a particular preferential orientation.

It is well-known that the employment of nanoscopic techniques to detect and characterize individual adsorbed proteins requires high control on substrate roughness, since single-molecule resolution can be obtained only if substrate roughness is much lower than typical protein size. The Au(111) surface completely fulfills such a requirement: by suitably exposing Au−glass substrates to a gas flame, atomically flat (111) terraces, over hundreds of nanometers, may be obtained, showing a typical roughness of about 0.1−0.05 nm (i.e., much lower than nanometer size of proteins). In the case of direct protein chemisorption, the annealed Au(111) substrate is incubated with biomolecule solution—typical concentration in the range of μM—at controlled temperature (usually 4 °C) for time ranging between minutes and hours, depending on the required surface coverage (from submonolayer to full coverage). After incubation, copious rinsing with buffer solution allows removal of any unadsorbed material from the substrate.

Besides the low roughness attainable by means of flame annealing, a gold surface also offers the advantage of very effective functionalization procedures, designed to modify the metal surface for optimal biomolecule immobilization. Several immobilization strategies have been proposed by many groups entailing the introduction of a spacer directly linked both to the metal surface and to the protein.[52,53]

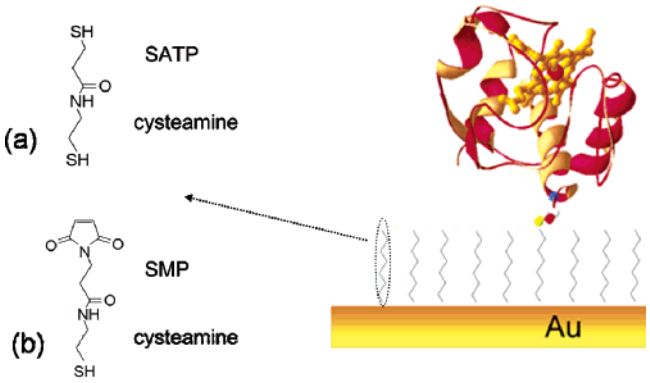

Figure 1. Schematic representation of two proposed immobilization strategies. Specifically, the Au(111) substrate is covered with (a) sulfhydryl- or (b) maleimide-terminated monolayer by first exposing the surface to a solution of cysteamine. Subsequent incubation with protein solution (YCC, in the figure) results in binding of the thiol-reactive end of the spacer with the sulfur atom of the exposed cysteine residue (Cys102 for YCC, represented in the figure with small spheres).

Here, we describe two examples experimented by our group, which resulted in being very effective, allowing immobilization of the protein in a preferential orientation and at a specific distance from the electrode. The observed retention of protein morphological characteristics,[56] the preserved biorecognition capability,[57] and the good electric conduction through the molecule toward the electrode,[56] provided by such immobilization strategies, are evidence of the optimal coupling between the biomolecule and the electrode. A schematic representation of the immobilization strategies proposed is shown in Figure 1. Specifically, the Au(111) substrates are covered with maleimide- or sulfhydryl-terminated alkanethiols by first exposing the surface to a solution of cysteamine (1 mM ethanolic solution for 15 h at room temperature); to get maleimide-terminated Au(111), the amino-terminated layer is subsequently incubated with a solution of *N*-succinimidyl 3-maleimidopropionate (SMP),[58] whereas, for the sulfhydryl termination, the modified substrate is incubated with a solution of *N*-succinimidyl-*S*-acetylthiopropionate (SATP).[59] In the first case, a simple rinsing (with *N*,*N*-dimethylformamide (DMF) and Milli-Q water) directly provide the maleimide-terminated Au(111). Conversely, the thiol-terminated Au is obtained only after deprotection of SATP sulfhydryl groups (see ref 57 for details); samples are subsequently rinsed with Milli-Q water. Then, the modified Au substrates are ready to covalently bind the metalloproteins through exposed cysteine residues (in the case of maleimide- or thiol-terminated Au) or disulfide moieties (for thiol-terminated substrates only), by simply incubating the sample with protein solution.

II.B. Detection Methodologies. In the past, protein adsorption on surfaces has been widely studied by means of ellipsometry,[60] surface plasmon resonance,[61] fluorescence spectroscopy,[62] or neutron reflectivity.[63] Even if these studies provided fundamental information on the investigated systems, most of these techniques often average signals from a large number of adsorbed molecules. Nanoscopic techniques allowed overcoming such a limit, greatly improving the detection sensitivity (down to single molecule), providing full characterization of individual adsorbed proteins in real time and without the need of any labels. In particular, novel operation modes of nanoscopy nowadays offer the possibility to sense single biomolecules by simply monitoring suitable features of the molecule, as for instance its morphology, or ET capability, conduction properties, or even its biorecognition capacity.

All scanning probe microscopy (SPM) techniques operate by scanning a sharp probe across a surface (eventually proteins adsorbed on a substrate) and simultaneously monitoring specific interactions with extremely high sensitivity. The first of these microscopes invented was the scanning tunneling microscope (STM),[64] capable of measuring a quantum mechanical tunneling current between a metallic tip, which is sharpened to a single atom point, and a conductive surface; since the rate of tunneling electrons depends sharply (exponentially) on the tip−sample distance,[65] the tip tracks the sample surface closely if the tunneling current is kept constant by a suitable feedback loop. The STM image, which is acquired by recording the variation of tip height while scanning the sample surface line by line, provides a final overall resolution of tenths of angstroms both in the vertical direction and in the sample plane. Actually, such an image is a combination of the topography and electronic properties of the sample.

The advent of atomic force microscopy (AFM)[66] allowed separating the morphological contribution from electronic properties. In AFM, the sharp tip is located at the end of a soft spring (cantilever) capable of sensing tip−sample interaction forces (such as electrostatic, van der Waals, frictional, capillary, and binding) as the tip approaches the sample. The tip−sample interactions result in cantilever deflections, easily detected by using a laser beam bouncing off the back of the cantilever onto a position-sensitive photodetector. AFM has an overall resolution in the vertical direction of tenths of angstroms, usually limited by thermal noise, and is capable of measuring ultrasmall forces (as small as piconewton). The resolution in the sample plane is generally limited by the tip radius of curvature and is a few nanometers; however, it can improve up to subnanometers when scanning 2D ordered arrays.[67] Traditionally, AFM has been used in contact mode, namely, measuring topography and friction by simply sliding the probe tip across the sample surface, keeping the tip in "physical contact" with the sample. Nevertheless, this operation mode may induce damaging of soft samples. Tapping mode AFM (TMAFM) allows overcoming problems associated with friction and adhesion, which may be critical when measuring biomolecules. In this configuration, shear forces are greatly reduced thanks to the intermittent contact between tip and sample.[68] The possibility to run TMAFM, as all SPM techniques, under an aqueous environment made this operation mode a powerful tool for the study of the morphological properties of biological samples.[69]

More recently, the employment of AFM also in the conductive mode configuration (CAFM) has been established. In CAFM, a bias is applied between an AFM conductive probe and the sample and the current flow is recorded while the pressure exercised by the probe is controlled by a feedback loop. In this way, topography, lateral forces, and current images are measured simultaneously, with the advantage that, in principle, conductive properties may be directly coupled to the sample morphology. However, only in a few cases restricted to inorganic and small molecules, the correlation between current images and structural features has been reported.[70−73] Specifically, the potentiality of this technique for sensing and characterizing single adsorbed biomolecules has been only moderately exploited.[74] Actually, the study of biomolecular conduction through single proteins has been mainly addressed by using a STM,[49,54,75] under electrochemical control[35,36,40,55,76,77] and by tunneling spectroscopy (STS);[40,78] in the latter configuration, the STM tip is held stationary over a single molecule and the current flow is measured as a function of the bias, after the feedback loop has been disengaged. Undoubtedly, so far,

this technique has provided a wide knowledge of the electron-transfer properties of metalloproteins; on the other hand, such a study of protein conduction suffers from the STM difficulty to establish a controllable tip−sample contact[79−81] (in STM, the current is used to control tip positioning, with consequent indetermination on tip vertical position). CAFM overcomes these difficulties, owing to the fact that current flow is recorded with the tip directly in contact with the sample, so that this technique emerges as a powerful tool to study the conduction properties of adsorbed biomolecules.

Among the different operation modes of nanoscopy which have great relevance to high-resolution biological sensing, there is STM-tip-enhanced Raman spectroscopy. Such an approach unifies STM with surface-enhanced Raman spectroscopy (SERS). In ordinary SERS, the huge Raman signal enhancement is obtained by adsorption of molecules onto nanometer-size metallic particles or rough metallic islands: together with an electromagnetic effect, responsible for the local field enhancement involving surface plasmon resonance, a charge transfer between the molecule and the metal surface has been suggested to contribute to SERS.[82,83] In STM-tip-enhanced Raman spectroscopy, the employment of a metal STM tip allows locating and localizing the large enhancement of the Raman scattering at the tip apex and its close vicinity. Usually, the target molecules are adsorbed on a planar surface, whereas the nanometer-sized tip is brought into optical contact with the adsorbate.[84,85] Here, we propose to adsorb the molecule on a metal STM tip whose roughness is suitable to dramatically enhance the molecule vibrational spectral emission.[86] By monitoring the SERS signal as well as the electron flow in the molecule−tip tunneling junction, the suggested approach offers the possibility to simultaneously investigate the vibrational and conductive properties of single molecules adsorbed on the STM tip.

In recent years, the additional potential of SPM for the study of intermolecular forces has gained great attention.[87] Indeed, the high force sensitivity (of the order of piconewtons)—peculiar of AFM—together with the optimal displacement resolution (0.1 nm), the small probe−sample contact areas (as small as 10 nm^2), and the ability to operate under physiological conditions render AFM an ultrasensitive detection tool for revealing biorecognition. Specifically, in atomic force spectroscopy (AFS), unbinding forces of single ligand−receptor pairs can be probed by recording force-versus-distance cycles on a surface-bound receptor by means of an AFM tip which has been functionalized with the ligand.[87] The ideal sensor configuration appears to be a single receptor covalently coupled to the tip via a flexible spacer molecule,[88] which leaves the ligand free to move and reorient for unconditioned recognition of the surface-bound receptor, favoring complex formation as the tip approaches the sample. With tip retraction, an increasing tensile force is applied to the complex, thereby reducing its lifetime until it dissociates at a measurable unbinding force. The characteristic stretching of the spacer preceding dissociation[89] helps to better discriminate specific unbinding events from unspecific adhesion. Furthermore, in the so-called dynamic force spectroscopy, by simply monitoring the complex unbinding force upon variations in the rate of applied force (loading rate), it is possible to get deeper insights into the molecular dynamics of individual recognition processes.[90−92] The additional possibility to measure adhesion force as a function of tip position over the substrate allows the generation of high-resolution affinity images.[93]

Thanks to all of the outstanding capabilities described here, it appears clear that SPM, with its variety of operation modes, emerges as a powerful ultrasensitive technique for detecting (and fully characterizing) single adsorbed biomolecules by simply monitoring the most suitable molecule characteristics (i.e., morphology, ET, conduction, vibrational properties, biorecognition, etc.). Interestingly, in the case of an ET protein electrically coupled with a conductive substrate (such as gold), the possibility to sense individual recognition events by, for instance, revealing very small variations in the conductive response would deserve challenging perspectives for novel detection modes which might be exploited in bioanalytics.

III. Detection of Single Metalloproteins Integrated with Metal Electrode

III.A. Morphological Properties. As widely discussed in a previous section, the combination of STM and AFM experiments may provide an accurate morphological characterization of single adsorbed proteins. As a matter of fact, TMAFM allows gaining a deeper insight into protein height and orientation above the substrate but provides only limited information about protein lateral dimensions (due to the relatively large size of the tip, which induces broadening effects in the biomolecule images[94]). Nevertheless, protein lateral dimension can be generally recovered by STM imaging,[35,36,40,49,78] which is known to induce a minor tip convolution and in some cases is even capable of revealing interesting submolecular features.[39,95] Here, both SPM modes have been employed to detect and fully characterize single metalloproteins chemisorbed on bare or modified gold electrodes. In particular, we examine the case of the azurin (AZ), which has been chemisorbed both on bare Au(111) and on sulfhydryl-terminated monolayers assembled on Au(111). This small redox copper protein bears an exposed disulfide bridge, located in a region opposite of the redox site,[96] which is suitable for covalent anchoring both on bare and thiol-terminated gold surfaces. Therefore, AZ molecules are expected to exhibit a similar orientation on the two substrates, with the main difference between the two configurations being the sheltering of protein residues from direct strong interaction with the metal substrate when a SAM is deposited on gold. Au modification was accomplished by cysteamine monolayer assembling followed by thiolation with SATP, as described in a previous section. Typical TMAFM images of AZ molecules directly chemisorbed on Au(111) substrate (sample AZ/Au) and on the thiol-terminated gold (sample AZ/SAM_SATP/Au) are shown in parts a and b of Figure 2, respectively. The molecules, which appear uniformly distributed over the substrate, are stably bound to gold, producing high-quality images even after repeated scans. Individual molecules are well resolved by this technique, and their height can be estimated with high resolution (0.1 nm) by analysis of the protein cross-section profile, shown in the figure. Such an analysis over hundreds of molecules provides a monomodal height distribution (not shown here)—see ref 37 for details—suggesting a preferential orientation of the protein over the substrate, with the mean molecular height being 1.7 nm, with a standard deviation of 0.6 nm. This value appears lower than values provided by X-ray crystallography,[96,97] as if a strong AZ interaction with gold either forces the protein to adopt a lying down configuration above the substrate or even causes a partial protein denaturation.[49] In contrast, for the AZ/SAM_SATP/Au sample, the monomodal height distribution is centered at a mean value of 3.4 nm, with a standard deviation of 0.8 nm, which well matches the crystallographic protein size.[56,96] These results indicate that, as expected, the interactions between the aminoacid residues and the noble metal are screened upon binding of AZ with the thiol group of the monolayer, and

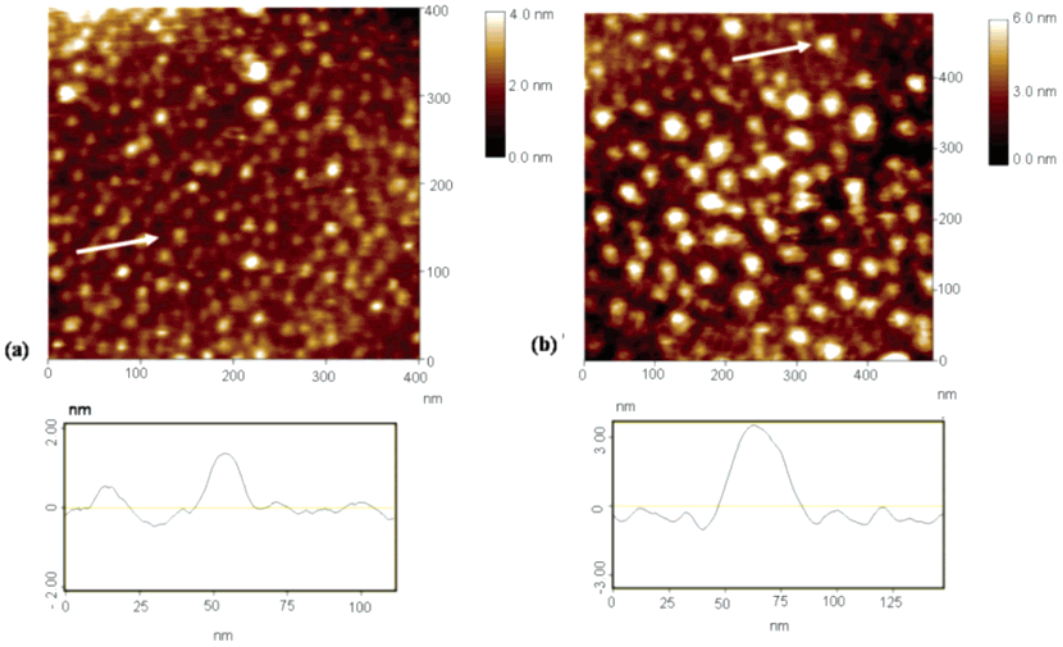

Figure 2. Typical TMAFM image of AZ molecules directly chemisorbed on Au(111) substrate (sample AZ/Au) (a) and on the thiol-terminated gold (sample AZ/SAM_SATP/Au) (b). The images are recorded in Milli-Q water. Cross-section profiles of the molecules indicated by arrows are shown below.

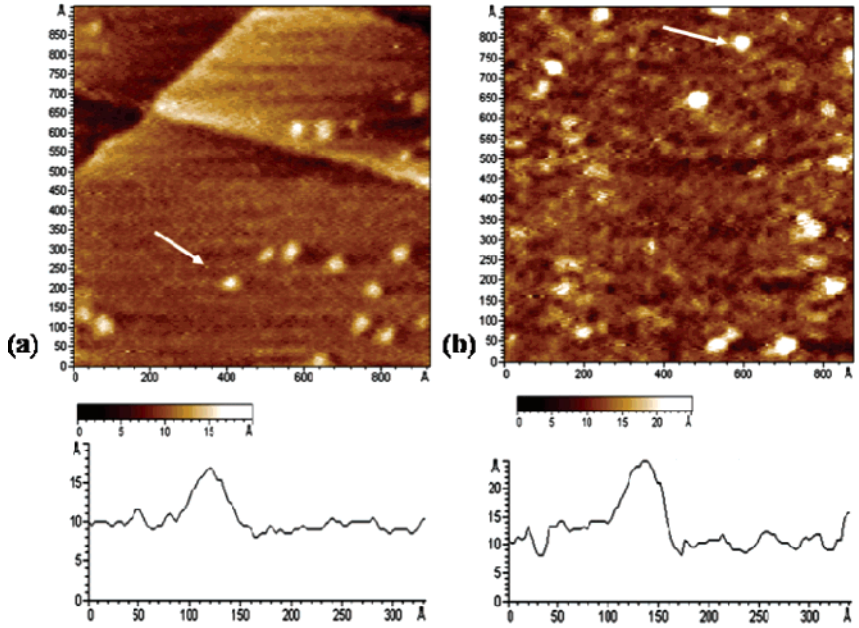

Figure 3. Representative STM images of AZ/Au (a) and AZ/SAM_SATP/Au (b) recorded in air. Tunneling current, 50 pA; bias, 0.2 V for image a and −0.9 V for image b. Cross-section profiles of the molecules indicated by arrows are shown below.

that under these conditions the protein may adopt a standing up configuration on the substrate with a three-dimensional structure closer to its native form.

Interestingly, a difference between the two samples is also found by STM. In Figure 3, representative STM images for both immobilization strategies are shown. Single AZ molecules can be well resolved over the substrate and appear as homogeneous globular shape structures. If the AZ lateral dimensions are very similar in the two samples (4.5 ± 0.9 and 3.7 ± 0.8 nm for adsorption on bare and modified gold, respectively, close to crystallographic values), this is not the case of the vertical size, which is found to be 0.5 ± 0.1 nm for AZ/Au and 1.8 ± 0.4 nm for AZ/SAM_SATP/Au. We recall here that, as discussed in the methodology section, STM images are a complex convolution of topographic and electronic contributions, so that the height of the biomolecule may deviate significantly from the purely topographic one; in particular, for proteins on conductive substrate, a reduced STM height—lower than molecule physical size—is usually observed, and has been generally related to the low conductivity of the biomolecules.[81] The (partial) recovery of STM height, as for AZ on modified gold, has been related to a more efficient electron tunneling through the protein when covalent immobilization is achieved by a suitable linker.[56]

A similar result has been also found for another redox protein, yeast cytochrome *c* (YCC). This protein has been directly chemisorbed on bare gold by means of a specific reaction between Au and the sulfur atom of an exposed cysteine residue (Cys102).[36] Alternatively the gold surface has been modified by deposition of SAMs, which were sulfhydryl- or maleimide-

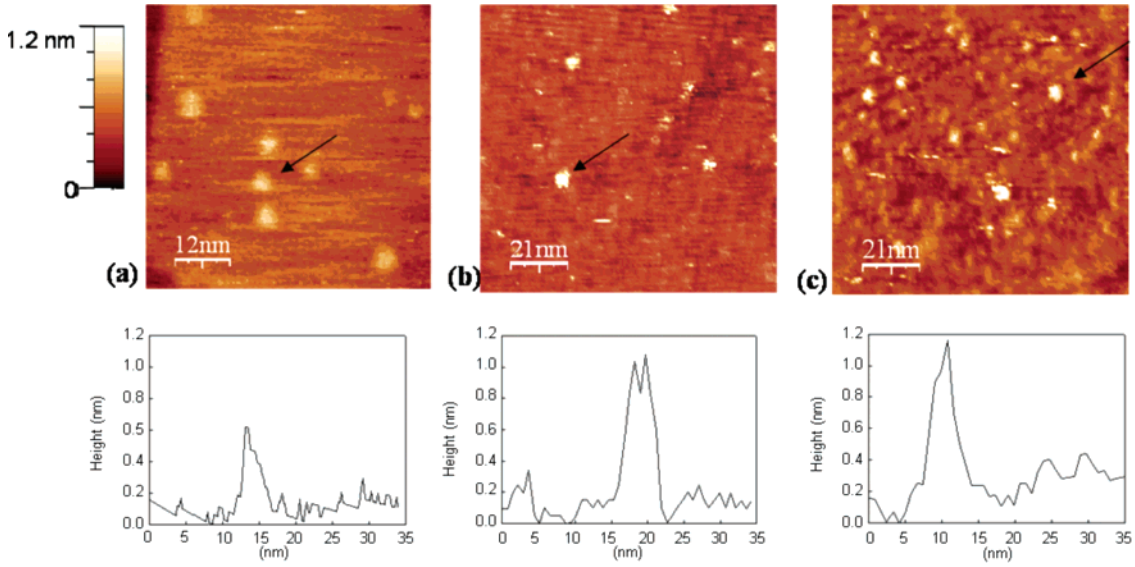

Figure 4. STM images of YCC molecules immobilized on bare gold (a) or on thiol-terminated (b) and on maleimide-terminated (c) monolayers assembled on Au(111) substrates. The images have been recorded in air at a tunneling current of 40−50 pA and at a bias of 0.2 V (a), −0.6 V (b), and −0.8 V (c). Cross-section profiles of the molecules indicated by the black arrows are shown below.

terminated (see the Materials section for details) in order to directly bind the free thiol of Cys102. The three samples display only small variations in the vertical size of proteins as measured by TMAFM imaging (not shown), with the mean measured height for YCC ranging from 2.6 ± 0.7 nm[36] (in the case of bare gold) to 3.9 ± 0.9 and 3.1 ± 0.7 nm for the sulfhydril- and maleimide-terminated SAM, respectively.[98] Interestingly, for the three immobilization strategies examined, the protein vertical size above the substrate was, within the error, very close to, or even in full agreement with, the molecule physical size as expected from crystallographic data (3.8 nm).[36] Conversely, a major difference among the three samples was observed when detecting the adsorbed molecules by STM imaging, as shown in Figure 4. As a matter of fact, the introduction of the spacer between the protein and the electrode determined an increased STM contrast of the biomolecules over the substrate, which resulted in almost doubling of the protein STM height; specifically, the protein height above the substrate, as estimated by cross-section profile analysis (see Figure 4) changed from about 0.4 ± 0.1 nm for YCC on bare Au to 0.8 ± 0.1 nm on the maleimide-terminated monolayer and 1.1 ± 0.6 nm on the thiol-terminated monolayer.[98] Therefore, as already discussed for AZ, also in this case, the introduction of a spacer between the protein and the electrode seems to favor the flow of tunneling current through the adsorbed biomolecule, somehow facilitating single-molecule detection by means of STM.

III.B. Electron-Transfer Capability and Spectroscopic Aspects. The possibility to perform STM imaging under electrochemical control (EC-STM) well applies to ET proteins. Indeed, such a STM configuration allows tuning the electrochemical potential to the protein redox midpoint potential. It has been shown that detectable changes in EC-STM image contrast, while sweeping the redox levels of the adsorbed metalloprotein, may provide fundamental information about possible contribution of redox levels in the tunneling mechanism.[99]

Notably, such an operation mode may have great relevance also to improve the sensitivity in the detection of biomolecules: an optimal working condition (corresponding to a precise substrate potential) may be found which, by increasing the STM contrast, helps in revealing the metalloprotein. As an example, we report here EC-STM results on a poplar platocyanin mutant (PCSS) adsorbed on a gold electrode. Chemisorption of the protein on the metal substrate was achieved via chemical binding between sulfur of exposed cysteine residues, introduced in the protein by genetic engineering,[55] and Au, as confirmed by the well resolved and stable AFM and STM imaging (not shown here), which on the other hand was not possible on analogous sample with the wild-type form of PC, lacking the S−S anchoring group.[40] Additionally, the well reproduced vertical and lateral size of the protein, as measured by means of TMAFM and STM, respectively, accounts for a nondenaturing adsorption of the macromolecule on the bare gold surface.[40] The PCSS/Au sample was further investigated by means of STM under electrochemical control: in this case, the use of a bipotentiostat allowed varying of the electrochemical potential of the sample in a wide range around the protein redox midpoint (+106 mV, referred to saturated calomel electrode (SCE)[55]). In Figure 5, representative EC-STM images are shown for the PCSS/Au sample. We can observe that the molecular features are clearly visible for substrate potential close to the protein midpoint potential (Figure 5a), whereas the image contrast appears weaker when the potential is far from this value (Figure 5b). Additional data, not shown here, also demonstrated the reversibility of such a mechanism, since, once the initial potential was re-established, the marked STM contrast could be recovered. A similar behavior has been observed also on other ET proteins, as for instance AZ. In that case, molecular features appeared like bright white spots in STM images when the substrate potential was close to the AZ redox midpoint; conversely, far from this value, a full bleaching of the spots occurred, resulting in a dramatic decrease of the detection sensitivity.[35,37]

A molecule put in close proximity of a metallic surface may also be investigated by SERS, as briefly described in the methodology section. If the metal surface where the molecule has been adsorbed is an STM tip, the electron flow in the molecule−tip tunneling junction can be examined as well. Possible advantages of such an approach are discussed here referring to experiments on a "model" system, namely, a simple molecule, iron−protoporphyrin IX (FePP), with ET capabilities. This molecule constitutes the prosthetic group of several metalloproteins, such as cytochromes, hemoglobin, and myoglobin, in which it plays a key role.

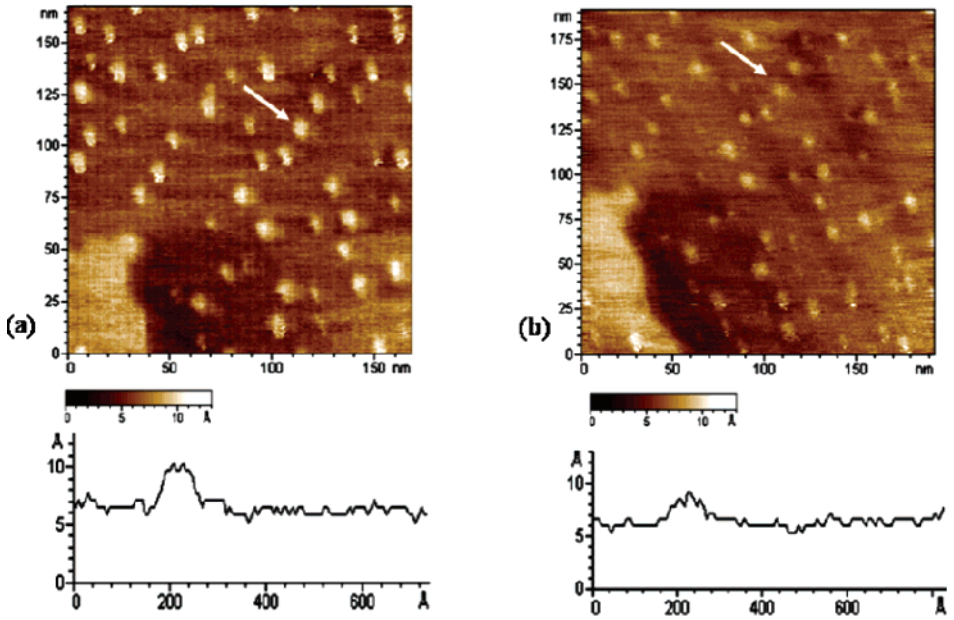

Figure 5. EC-STM images of the PCSS/Au sample for a substrate potential set at +28 mV vs SCE (a) and +222 mV vs SCE (b). Tunneling current, 50 pA; bias, 0.180 V. Cross-section profiles of the molecules indicated by the arrows are shown below.

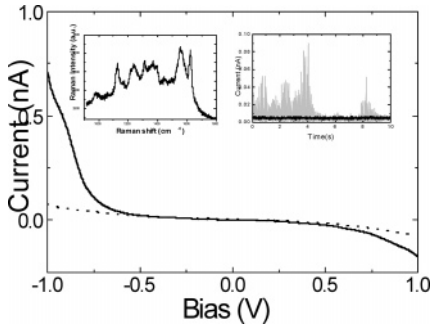

Figure 6. $I-V$ curve recorded with the STM tip incubated with FePP and brought against a conductive substrate (HOPG) (continuous line). For comparison, a $I-V$ curve recorded with a bare STM tip is also shown (dashed line). Left inset: spectrum by collecting 100 SERS spectra from a silver tip incubated with FePP at 10^{-9} M in temporal sequence, with each spectrum being obtained with 1 s of integration time. Right inset: tunneling current, at a fixed bias of 0.2 V, as a function of time, for a bare tip (black curve) and for a silver tip incubated with FePP (gray curve).

To perform SERS/STM combined experiments, the molecules have been adsorbed on an STM silver tip whose roughness is suitable to hugely enhance the molecule vibrational spectral emission at the single-molecule level.[86] In the left inset of Figure 6, the spectrum from a silver tip incubated with FePP at 10^{-9} M displays the main vibrational features of FePP, fully described in the literature.[100] Nevertheless, sequences of SERS spectra (each recorded, by means of a CCD, with a 1 s integration time) exhibit drastic and rapid intensity and spectral fluctuations, typical of systems in the single-molecule regime. Interestingly, the vibrational peaks at 1363 and 1375 cm^{-1}, corresponding to vibrational markers of ferrous and ferric iron states, respectively, are randomly and alternatively detected in the sequence of spectra. Such a behavior, already observed for FePP on silver colloids,[101] can be put into relationship to fast and reversible changes in the oxidation state of the FePP iron ion during the measurements. An ET process can then be invoked, with the molecule being assumed to undergo a nonradiative process where ballistic electrons from the silver surface could jump toward the FePP molecule and backward.[102] Therefore, even if we cannot exclude that interfacial molecule−metal interactions might assist such an ET process, it could be quite reasonable that the energy required to overcome the barrier between the two oxidation states could be provided by light excitation.[29]

The strong electronic coupling between the molecule and the metal, as indicated by the switching between iron oxidation states, suggests the investigation of the electron flow through an STM tip−FePP tunneling junction. To this aim, the STM tip incubated with FePP was brought against a conductive substrate (HOPG) and the current was measured as a function of bias voltage. The $I-V$ curve, shown in Figure 6, appears markedly asymmetric, increasing at negative bias, whereas the tunneling curve for the bare silver tip is highly symmetric. Generally, a diode-like trend for the $I-V$ curve[103,104] reflects the redox properties of the molecule;[99] in particular, consistently with Schmickler theory,[104] an extra current monitored by means of STS may result from tunneling via oxidized states on the molecule as the bias voltage is made more negative. Bearing in mind the switching observed in SERS spectra, we monitored the tunneling current, at a fixed bias, as a function of time (Figure 6, right inset). Drastic fluctuations of the current were observed with the FePP tip, reminiscent of the fluctuations found in SERS spectra, whereas an almost constant current is monitored with a bare tip. Such behavior, observed for different FePP−tip systems and for different applied biases, is indicative of a significant variability in the tip−molecule−substrate junction occurring during the tunneling experiments. It has been observed that injection of tunneling electrons by an STM tip on a porphyrin molecule can excite its vibrational modes, eventually leading to diffusive processes.[105] This provides some evidence for a coupling between electronic and vibrational properties at the level of single molecule; more specifically, the combined STS/SERS results reported here can be interpreted in terms of continuous, random changes of the spatial arrangements of the molecule at the metal interface, which are likely to affect the ET properties of the molecule.[86] The chance, here shown, to simultaneously investigate vibrational and conductive properties of molecules via adsorption on a metal tip deserve

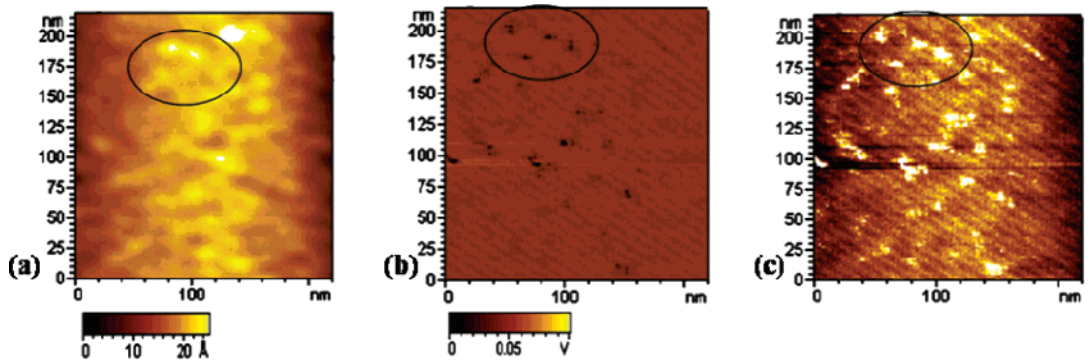

Figure 7. Topography and current images of PCSS molecules chemisorbed on Au(111) substrates under a nitrogen atmosphere. Part a shows a topography image acquired at a −0.8 V bias and 300 pN of applied load, part b shows the corresponding current image, and part c has been obtained by subtracting image a from image b.

interesting perspectives in view of gaining deeper insight into the ET capability of the single molecules adsorbed on a metal surface.

III.C. Electric Coupling of Single Metalloproteins with the Electrode. Electric coupling of ET proteins with a metal electrode may be investigated by means of CAFM. Indeed, as already discussed in the Methods section, this operation mode allows placing the tip directly in contact with the adsorbed molecule and monitoring the current flow through the molecule toward the electrode, once a specific bias voltage has been applied between them. Additionally, by this technique, it is possible to simultaneously record topography and current images so that a direct correlation between structural features and electrical characteristics of the adsorbed single biomolecules can be investigated. The "trial" sample reported here, which has been examined by means of CAFM, is PCSS/Au (already discussed in the framework of ECSTM detection). In practice, a conductive AFM probe was approached down to contact the PCSS monolayer assembled on the Au(111) substrate; both lever deflection and current signal were monitored. Due to the experimental conditions (such as the tip radius and size of the molecule), the conduction properties of a few molecules, possibly only one, are investigated. Figure 7 shows a representative topography image recorded on a PCSS monolayer at negative bias (Figure 7a) and the corresponding current image (Figure 7b). The assembled proteins can be discerned in the topography, even if the image is slightly perturbed. This effect is likely due to electrostatic forces, which add to mechanical load (typical of contact mode operation) when a bias is applied between the tip and the substrate. The reduced protein vertical size (less than 1 nm, lower than that obtained in TMAFM[40] and by crystallography[106]) has to be ascribed to the pressure exercised by the tip during the scan in contact mode as well as to the high density of molecules, which complicates the measurement of the vertical size of a single protein. Regarding the current image, dark spots with intensities comprised between 10 and 100 pA can be detected for negative bias (it is worth noticing that in current images recorded at negative bias the darker are the spots the more conductive is the object). If comparing current image to topography, a good correlation between current spots and morphological features can be found for some molecules (the circles in the figure indicate molecules and spots where the correlation seems more clear). Figure 7c provides a clear indication that an exact correspondence of the features occurs. This figure has been obtained by subtracting current image from the associated topography; the resulting image displays spots, which overlap the molecules observed in topography, eventually emerging as brighter features. Notably, despite the fact that the PCSS monolayer is clearly distinguished

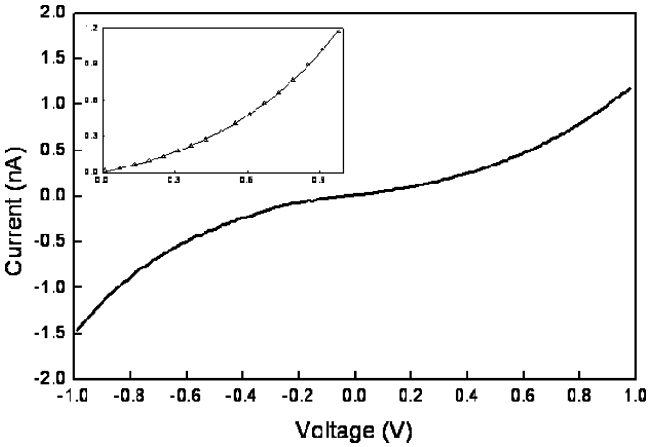

Figure 8. $I-V$ curve on PCSS anchored on gold as measured by CAFM at an applied load of 3 nN. Inset: fitting curve (straight line) of the experimental $I-V$ curve (triangles). Only one experimental value every four is shown for clarity. Measurements were carried out under a dry nitrogen atmosphere.

in the topographical image recorded at positive bias, no current signal is detected under such experimental conditions. The observed behavior can be ascribed to a possible charging effect due to scanning of the metal coated tip on the protein surface, which blocks current flow at this polarity. Indeed, a similar phenomenon was found in CAFM imaging of semiconductor nanocrystals inserted into a thin polymer film.[72]

If the tip is not scanned across the protein surface but is kept at a fixed position, the conduction through a single PCSS protein chemically bound to the metal electrode can be investigated. Specifically, once the contact resistance between the tip and the protein is overcome (by applying a suitable force), the current tunnels from the tip toward the substrate—or vice versa, depending on the bias polarity—through the protein and $I-V$ curve, as that shown in Figure 8 for PCSS/Au can be recorded. The experimental data reveal an efficient conduction through the molecule toward the conductive substrate, as on the other hand expected for a covalent linkage to gold, thus assessing good coupling to the metal electrode.

A theoretical model has been proposed in order to quantitatively describe the conduction across the tip−protein−substrate tunneling junction, which allows one to single out the electron transport properties of the macromolecule.[74] In the model, the current is written as $I = VG$, where G is the conductance given by the Landauer formula, $G = (2e^2/h)T_{tot}$. The term T_{tot} represents the total electron transmission probability from the electrode to the tip and is obtained as the product of the transmissions of the different components, namely, the protein−

electrode chemical bond (T_{SS-Au}), the molecule ($T_{protein}$), and the physical contact between the protein and the tip (T_{tip}), so that $T_{tot} = T_{SS-Au}T_{protein}T_{tip}$. The experimental evidence that a good electric contact is attained between the tip and the molecule as well as between the molecule and the electrode allows treating both T_{SS-Au} and T_{tip} as a constant.[74] On the other hand, the electron transport through the macromolecule can be described as a coherent nonresonant tunneling through a rectangular barrier of height $\varphi_{protein}$ and length $L_{protein}$; therefore, the transmission probability through the protein can be written as $T_{protein} = \exp(-\beta_{protein}L_{protein})$, where $\beta_{protein}$ represents the decay constant reflecting the strength of electronic coupling across the barrier and has the expression $\beta_{protein} = (4\pi/h)[2m^*(\varphi_{protein} - eV)]^{1/2}$, with V being the applied bias and m^* the effective electron mass, which for the examined PCSS/Au sample is made equal to 0.16 m, following refs 35, 80, and 81. The theoretical model described here has been demonstrated to well reproduce the experimental $I-V$ curves, as that shown in Figure 8 for PCCS (see the inset of the figure), also providing for the fitting parameters, $\varphi_{protein}$, $L_{protein}$, and $\beta_{protein}$, values which are independent of the applied load.[74] Such behavior has also been observed in other metalloproteins[49,54] and indicates that structural and conduction properties of the adsorbed protein are not affected by applying a load (at least in the range explored). The theoretical approach described here, which can be extended to various molecules, represents an advancement in understanding the conduction properties of biomolecules covalently bound to a gold surface and provides more insight into the electric coupling between the macromolecule and the electrode.

IV. Sensing the Biorecognition Capability of Gold-Immobilized Metalloproteins

In a previous section, we have shown how detection (and characterization) of single adsorbed redox proteins may be achieved by monitoring different parameters as, for instance, topography, ET, and conduction. Here, we discuss sensing of functional metalloproteins, adsorbed on a conductive substrate, by revealing their biorecognition capability.

The couple of redox partners examined here is AZ−cytochrome *c*551 (C551). The interaction between these two ET proteins is believed to occur through different steps:[107] after protein recognition and specific binding, ET between the two partners can take place with optimal efficiency; the complex subsequently dissociates to yield the products.

The biorecogniton between gold-immobilized AZ and C551 is investigated at the single-molecule level by atomic force spectroscopy (AFS). Since the first experiments on biotin−avidin,[108] AFS has been widely demonstrated to represent an extremely powerful tool for sensing single-molecule interaction, for instance, in antigen−antibody pairs or in the formation of protein−DNA complexes, or even between complementary DNA strands.[109] Nevertheless, it is worth stressing that the study of redox partner interaction by means of this technique represents a novelty, and to the best of our knowledge, the case of an ET complex was the first discussed in the literature.[110]

In order to optimize partner interaction, the biomolecules have been linked to substrate and tip with proper orientation, namely, by taking into account the protein residues involved in the interaction (as obtained by means of site-directed mutagenesis experiments[111]); also, the expected configuration of the AZ−C551 complex (as from computational docking simulations) is considered, this being in agreement with the cited experiments.[112] Specifically, AZ has been immobilized on bare or modified gold via the disulfide bridge, thus orienting the protein

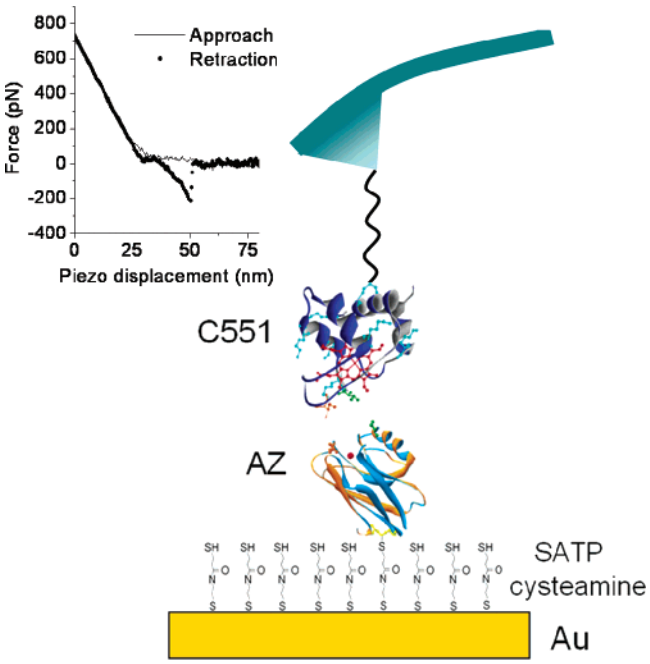

Figure 9. Schematic representation of the AFS setup: AFM tip functionalized with C551 via the PEG cross-linker and AZ immobilized on gold modified by deposition of cysteamine−SATP SAM. Inset: representative force-versus-distance cycle recorded in PBS buffer solution, showing PEG stretching and following C551−AZ unbinding.

to a configuration in which the hydrophobic patch, involved in the interaction with C551, is placed toward the AFM tip.[96,111] The electrode modification was obtained by deposition of thiol-terminated SAM, as described in the Materials section. Conversely, C551 molecules have been adsorbed on the AFM tip through a few-nm-long cross-linker, a polyethylene glycol (PEG) derivative, which allows protein reorientation over the AZ sample, thus facilitating the mutual interaction; the PEG solution was adjusted to ensure a low density of cross-linkers on the tip surface, and possibly single-molecule detection by the tip.[113] A schematic representation of the experimental setup with the C551-functionalized tip and the AZ/SAM/Au sample is shown in Figure 9.

Prior to force spectroscopy experiments, adsorption of AZ molecules on bare and modified gold was checked by TMAFM and STM imaging. The imaging tip was then replaced with the C551-functionalized tip for force spectroscopy measurements in the contact mode. A representative force-versus-distance cycle recorded on the AZ/SAM/Au sample is shown in the inset of Figure 9. Similar curves were also observed on the AZ/Au sample. The retrace curve displays the characteristic nonlinear behavior of PEG linker stretching, in accordance with the wormlike chain polymer-elasticity model;[114] subsequent AZ−C551 unbinding is detectable as a pull-off jump. The experimental unbinding probability was about 18% for AZ on bare gold, whereas a lower value (9%) was found for the AZ/SAM/Au sample, consistent with the lower AZ coverage of the modified substrate, as evidenced by TMAFM and STM imaging[57] (not shown). The statistical distribution of the unbinding forces, measured as the force at the pull-off jump, is found to be mostly monomodal (see, for instance, the inset of Figure 10), so that detection of multiple bindings may be ruled out.[108] A control experiment was performed by employing a bare tip. In this case, no pull-off jumps were detected, except for some which were preceded by a linear dependence of force versus distance, characteristic of nonspecific adhesion. Also, the length scale of these jumps, 7 ± 2 nm, was consistent with typical

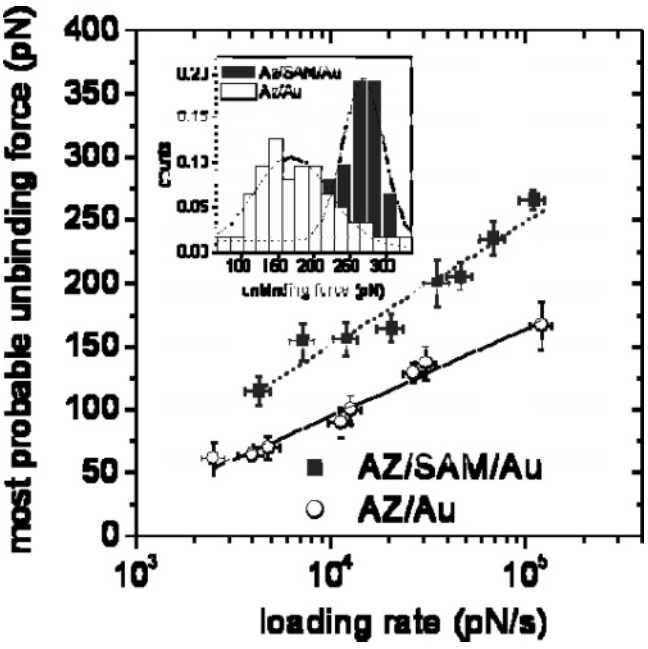

Figure 10. Most probable unbinding force of C551−AZ (determined by fitting a Gauss distribution to the histogram of the measured forces, as shown in the inset for the highest loading rate) plotted as a function of loading rate. Open and full symbols refer to AZ molecules immobilized on bare gold (sample AZ/Au) and on the modified substrate (sample AZ/SAM/Au), respectively. The lines correspond to a numerical fit of experimental data to the Bell model, as described in the text.

distances of adhesion,[115] whereas it was much lower than the typical unbinding length recorded with the PEG−C551-functionalized tip (23 ± 7 nm, as expected for PEG stretching and following C551−AZ unbinding[114]). To further validate the specificity of the detected unbinding events, as that shown in the inset of Figure 9, control experiments were also performed in a condition where AZ−C551-tip recognition was inhibited. This is usually achieved by addition of a blocking agent in the fluid cell;[116] in the present case, free AZ solution was added, in order to saturate the C551 proteins on the AFM tip. A significant decrease (about 65−70% lower than the initial value) of the unbinding probability was observed. The persistence of a residual unbinding activity (corresponding to an unbinding probability of a few percent) is common to numerous blocking experiments performed on different systems, even in very effective blocking conditions, namely, with a huge excess of the blocking agent, and has often been related to the forced interaction between ligand and receptor, due to the peculiar experimental setup.[110,116,117] The relevance of data discussed here is evident, since they demonstrate, at the single-molecule level, that biorecognition capability between the two ET partners is preserved even when one of them is adsorbed on a metal electrode.

This kind of experiments, performed by means of AFS, may even help establishing if the effectiveness of molecular recognition may be improved by means, for instance, of a suitable immobilization strategy of the ET protein on the conductive substrate. Experiments performed at different loading rates (namely, at different scan rates of the AFM tip in the retraction curve) may offer this possibility. Indeed, such an AFS operation mode, commonly called dynamic force spectroscopy, provides unique information about the unbinding kinetics of a single complex, also allowing the determination of the dissociation rate.[91,118] Such an analysis has been applied to AZ−C551, with AZ immobilized either on bare or modified gold. In Figure 10, the most probable unbinding force (determined by fitting a Gauss distribution to the histogram of the measured forces, as shown in the inset of the figure for maximum loading rate) is plotted as a function of the loading rate for both systems investigated. We can notice that the AZ−C551 rupture forces in the case of AZ/SAM/Au are higher that those measured for AZ/Au. Indeed, in the range of loading rates explored, the most probable AZ−C551 unbinding force increases from 114 to 267 pN for AZ/SAM/Au, whereas it goes from 65 to 165 pN for AZ/Au. The progressive increase of the force, with almost a linear trend versus the logarithm of the loading rate, suggests that these data can be examined in the context of Bell's model,[90] which treats the unbinding process of a ligand−receptor pair under the influence of an external loading force as a kinetic problem of escape from a potential well. According to this model, successfully applied to several complexes, the most probable unbinding force, F^*, can be written as $F^* = (K_BT/x) \ln[(\nu x)/(K_BTk_{off})]$, where K_B is Boltzmann's constant, T is the temperature, x is a parameter related to the length scale of the interaction, ν is the loading rate, and k_{off} is the dissociation rate in the absence of applied force. The off-rate values found by fitting the experimental data plotted in Figure 10 are 6.7 ± 2.3 s^{-1} for AZ adsorbed on modified gold and 14 ± 2 s^{-1} if AZ is directly immobilized on bare gold. Both values are much higher than typical off-rates estimated by dynamic force spectroscopy for "stable" ligand−receptor pairs (as for instance biotin−avidin or antigen−antibody);[119−122] this is indicative of a quite fast complex dissociation, consistent with the transient nature of ET complexes.[107,123] Interestingly, the significantly lower dissociation rate of the AZ−C551 complex in the case of AZ on modified gold (about half of the value estimated for AZ on bare Au) indicates that AZ molecules fit more tightly to C551 when linkage to the conductive substrate is accomplished via a spacer. As a matter of fact, the linker introduced between the biomolecule and the metal electrode is likely to leave the protein free to move and reorient for optimal interaction with its counterpart, resulting in a rise of binding affinity; also, the higher values observed for rupture forces when protein immobilization is achieved via a spacer is consistent with such a finding.

The fitting procedure shown in Figure 10 also provides an estimate for the potential barrier width between the complex bound and transition state,[90] indicated in Bell's equation with x. Since, in general, a smaller potential barrier width reflects protein resistance against bond rupture,[124] the slightly lower value of x for AZ immobilized via the spacer (0.098 ± 0.009 nm, to be compared with 0.14 ± 0.01 nm estimated for AZ on bare Au) is consistent with lower values of k_{off} as well as with the higher forces observed, with all the findings indicating a more effective molecular recognition of the redox partners when immobilization on gold is achieved via a linker.

The experimental results discussed here give evidence that AFS may be successfully applied to sense biorecognition not only in well-established cases,[125] as for instance antigen−antibody, or protein−DNA complexes, but also between two redox partners, even disclosing unique information about their interaction.

V. Conclusions and Outlook

In the present article, we have focused on the integration of functional biomolecules with conductive substrates, a subject which plays a central role in the fabrication of biodevices constructed at the nanometer scale. In particular, we have dealt with redox proteins, since they possess unique characteristics

(such as ET capability, possibility of gating redox activity, nanoscale dimension), which render them appealing for incorporation in hybrid systems.

The ability to create a controlled and optimized connection between a functional ET protein and a metallic electrode, and possibly to convert a biological function into a detectable signal, represents a challenging issue in view of applications in nanobiosensing. It is clear that a fundamental step in this direction is the full characterization of the adsorbed proteins in terms of functionality, as well as topological and conductive properties, at the single-molecule level.

In this framework, the integration of ET proteins with metal electrodes has been deeply investigated in the present article by means of a multitechnique approach—based on several SPM operation modes also combined with SERS—which is capable of providing a widespread characterization of single adsorbed molecules. Different metalloproteins have been examined, showing for each protein some particular characteristics which have been deeply analyzed. The results discussed in the present article are aimed at pointing out the potentiality of a multitechnique approach for exploring similar systems rather than fully characterizing a specific sample.

Specifically, we have demonstrated how the success of an immobilization strategy for the integration of proteins with gold electrode can be promptly assessed by the proposed approach. In this respect, the preserved morphology of biomolecules immobilized via a specific substrate functionalization may be verified by AFM and STM imaging; the latter operation mode also offers unique information about possible enhancement of tunneling current through the molecules (owing, for instance, to a specific immobilization strategy) as for a more efficient electrical coupling between the ET protein and gold. We have also shown that conduction through the molecule toward the electrode, with the probe (tip) in physical contact with the adsorbed molecule, may be monitored—as a function of the applied bias—by means of CAFS; a theoretical model has been reviewed which well describes the experimental data of current flow in the tip−protein−substrate junction, thus allowing one to gain more insight into conduction properties of gold-immobilized biomolecules.

We have also shown that, thanks to the employment of AFS, it is possible to assess if molecular recognition between two redox partners is preserved, even when one of them is linked to a metal electrode. For the redox couple examined in the article, the preserved biorecognition capability is clearly demonstrated even upon adsorption of one of the partners on gold. Additionally, by means of such an operation mode, we were also able to establish that a specific immobilization strategy, which was found to favor the protein−substrate electrical coupling, also facilitates the interaction of the adsorbed metalloprotein with its counterpart, thus favoring biorecognition.

Besides the characterization facet, the proposed multitechnique approach also deserves major potentialities for ultrasensitive detection of adsorbed biomolecules. Indeed, we have discussed how the complementary employment of the proposed techniques may optimize sensing of single biomolecules by simply recording the most appropriate among different types of signal. For example, we have seen that operation of STM under electrochemical control, besides providing fundamental information about possible contribution of redox levels in the tunneling mechanism, also offers the possibility to increase the STM contrast, thus facilitating molecule detection. The possible combination of STM with SERS (as reported in the article for a trial ET molecule) may offer the additional chance to reveal single molecules by monitoring their vibrational features, also yielding a chemical fingerprint.

Similarly, operation of AFM in the conductive mode not only may provide more insight into the conduction properties of ET proteins coupled to a metal electrode (as from the $I-V$ characterization previously discussed) but also suggests the possibility to detect the adsorbed macromolecules by recording a spatially resolved current image, which is directly related to the protein topography.

A novel aspect discussed in the present article, which is noteworthy since it may deserve challenging perspectives in the field of nano-biosensing, is the preserved biorecognition of a single ET protein by its gold-immobilized redox partner, as demonstrated by our AFS results. Actually, the employment of a gold substrate in AFS experiments has also been proposed by other groups for various biomolecules;[126−128] however, such a choice was mainly driven by the need to firmly attach the proteins to the solid support, for instance, by exploiting the affinity that sulfur has for gold. On the contrary, so far, little attention has been devoted to possible advantages that a conductive substrate may offer, provided that the biorecognition capability of the single adsorbed molecule is preserved and an electrical coupling with the electrode is established. Indeed, if this is the case, as demonstrated in this article for some ET proteins, the described approach may be an optimal starting point for advanced applications of these molecules in ultrasensitive biosensors, eventually based on detecting individual molecular recognition events, for example, as a measurable electric signal.

Acknowledgment. This work has been partially supported by Innesco-CNISM project 2005 and two PRIN-MIUR 2006 projects (nos. 2006028219 and 2006027587). L.A. acknowledges the Research Grant MUR "Brain Gain Project".

References and Notes

(1) Willner, I.; Willner, B. *Trends Biotechnol.* **2001**, *19*, 222.
(2) Willner, I. *Science* **2002**, *298*, 2407.
(3) Lowe, C. *Curr. Opin. Struct. Biol.* **2000**, *10*, 428.
(4) *Bioelectronics: From Theory to Applications*; Willner, I., Katz, E., Eds.; Wiley-VCH Verlag GmbH & Co. KGaA: Weinheim, Germany, 2005.
(5) Jianrong, C.; Yuqing, M.; Nongyue, H.; Xiaohua, W.; Sijiao, L. *Biotechnol. Adv.* **2004**, *22*, 505.
(6) Jain, Kewal K. *Clin. Chim. Acta* **2005**, *358*, 37.
(7) Nakamura, H.; Karube, I. *Anal. Bioanal. Chem.* **2003**, *377*, 446.
(8) Rosi, N. L.; Mirkin, C. A. *Chem. Rev.* **2005**, *105*, 1547.
(9) Albrecht, C.; Blank, K.; Lalic-Mülthaler, M.; Hirler, S.; Mai, T.; Gilbert, I.; Schiffmann, S.; Bayer, T.; Clausen-Schaumann, H.; Gaub, H. E. *Science* **2003**, *301*, 367.
(10) Ruckstuhl, T.; Enderlein, J.; Jung, S.; Seeger, S. *Anal. Chem.* **2000**, *72*, 2117.
(11) Blank, K.; Mai, T.; Gilbert, I.; Schiffmann, S.; Rankl, J.; Zivin, R.; Tackney, C.; Nicolaus, T.; Spinnler, K.; Oesterhelt, F.; Benoit, M.; Clausen-Schaumann, H.; Gaub, H. E. *Proc. Natl. Acad. Sci. U.S.A.* **2003**, *100*, 11356.
(12) Yi Cui, Y.; Wei, Q.; Park, H.; Lieber, C. M. *Science* **2001**, *293*, 1289.
(13) Chen, R. J.; Bangsaruntip, S.; Drouvalakis, K. A.; Wong Shi Kam, N.; Shim, Yiming Li, M.; Kim, W.; Utz, P. J.; Dai, H. *Proc. Natl. Acad. Sci. U.S.A.* **2003**, *100*, 4984.
(14) Ghindilis, A. L.; Atansov, P.; Wilkins, M.; Wilkins, E. *Biosens. Bioelectron.* **1998**, *13*, 113.
(15) Willner, I.; Katz, E. *Angew. Chem., Int. Ed. Engl.* **2000**, *39*, 1180.
(16) Delamarche, E.; Sundarababu, G.; Biebuyck, H.; Michel, B.; Gerber, C.; Sigrist, H.; Wolf, H.; Ringsdorf, H.; Xanthopoulos, N.; Mathieu, H. *Langmuir* **1996**, *12*, 1997.
(17) Disley, D. M.; Cullen, D. C.; You, H. X.; Lowe, C. R. *Biosens. Bioelectron.* **1998**, *13*, 1213.
(18) Mirski, V. M.; Riepl, M.; Wolfbeis, O. S. *Biosens. Bioelectron.* **1997**, *12*, 977.
(19) Patel, N.; Davies, M. C.; Hartshorne, M.; Heaton, R. J.; Roberst, C. J.; Tendler, S. J. B.; Williams, P. M. *Langmuir* **1997**, *13*, 6485.
(20) Katz, E.; Willner, I. *ChemPhysChem* **2004**, *5*, 1084.

(21) Willner, I.; Willner, B.; Katz, E. *Bioelectrochemistry* **2007**, *70*, 2.
(22) Lösche, M. *Curr. Opin. Solid State Mater. Sci.* **1997**, *2*, 546.
(23) Nazin, G. V.; Qui, X. H.; Hom, W. *Science* **2003**, *302*, 77.
(24) Castner, D. G.; Ratner, B. D. *Surf. Sci.* **2002**, *500*, 28.
(25) Gilardi, G.; Fantuzzi, A. *Trends Biotechnol.* **2001**, *19*, 468. Gilardi, G.; Fantuzzi, A.; Sadeghi, S. J. *Curr. Opin. Struct. Biol.* **2001**, *11*, 491.
(26) Gittins, D. I.; Bethell, D.; Schiffrin, D. J.; Nichols, R. J. *Nature* **2000**, *408*, 67.
(27) Loppacher, Ch.; Guggisberg, M.; Pfeiffer, O.; Meyer, E.; Bammerlin, M.; Lüthi, R.; Schlittler, R.; Gimzewski, J. K.; Tang, H.; Joachim, C. *Phys. Rev. Lett.* **2003**, *90*, 066107.
(28) Xiao, Y.; Patolsky, F.; Katz, E.; Hainfeld, J. F.; Willner, I. *Science* **2003**, *299*, 1877.
(29) Adams, D. M.; Brus, L.; Chidsey, C. E. D.; Creager, S.; Creutz, C.; Kagan, C. R.; Kamat, P. V.; Lieberman, X. M.; Lindsay, S.; Marcus, R. A.; Metzger, R. M.; Michel-Beyerle, M. E.; Miller, J. R.; Newton, M. D.; Rolison, D. R.; Sankey, O.; Schanze, K. S.; Yardley, J.; Zhu, X. *J. Phys. Chem. B* **2003**, *107*, 6668.
(30) Bizzarri, A. R.; Cannistraro, S. In *Encyclopedia of Condensed Matter Physics*; Elsevier: Heidelberg, 2005.
(31) Sigfridsson, K.; Ejdeback, M.; Sundahl, M.; Hasson, O. *Arch. Biochem. Biophys.* **1998**, *351*, 197.
(32) Haehnel, W.; Jansen, T.; Gause, K.; Klösgen, R. B.; Stahl, B.; Michl, D.; Huvermann, B.; Karas, M.; Hermann, R. G. *EMBO J.* **1994**, *13*, 1028.
(33) Whitesides, G. M.; Mathias, J. P.; Seto, C. T. *Science* **1991**, *254*, 1312.
(34) Ferretti, S.; Paynter, S.; Russell, D. A.; Sapsford, K. E.; Richardson, D. J. *Trends Anal. Chem.* **2000**, *19*, 530.
(35) Facci, P.; Alliata, D.; Cannistraro, S. *Ultramicroscopy* **2001**, *89*, 291.
(36) Bonanni, B.; Alliata, D.; Bizzarri, A. R.; Cannistraro, S. *ChemPhysChem* **2003**, *4*, 1183.
(37) Bonanni, B.; Alliata, D.; Andolfi, L.; Bizzarri, A. R.; Cannistraro, S. In *Surface Science Research Developments*; Norris, C. P., Ed.; Nova Science Publishers: New York, 2005; p 1.
(38) Davis, J. J.; Morgan, D. A.; Wrathmell, C. L.; Zhao, A. *IEEE Proc. Nanobiotechnol.* **2004**, *151*, 37.
(39) Friis, E. P.; Andersen, J. E.; Kharkats, Y. I.; Kuznetsov, A. M.; Nichols, R. J.; Zhang, J. D.; Ulstrup, J. *Proc. Natl. Acad. Sci. U.S.A.* **1999**, *96*, 1379.
(40) Andolfi, L.; Bonanni, B.; Canters, G. W.; Verbeet, M. Ph.; Cannistraro, S. *Surf. Sci.* **2003**, *530*, 181.
(41) Andolfi, L.; Canters, G. W.; Verbeet, M. Ph.; Cannistraro, S. *Biophys. Chem.* **2004**, *107*, 107.
(42) Weisshaar, D. E.; Lamp, B. D.; Porter, M. D. *J. Am. Chem. Soc.* **1992**, *114*, 5860.
(43) Ulman, A. *Chem. Rev.* **1996**, *96*, 1533.
(44) Nuzzo, R. G.; Zegarski, B. R.; Dubois, L. H. *J. Am. Chem. Soc.* **1987**, *109*, 733.
(45) Zhou, Y.; Nagaoka, T.; Zhu, G. *Biophys. Chem.* **1999**, *79*, 55.
(46) Reed, D. E.; Hawkridge, F. M. *Anal. Chem.* **1987**, *59*, 2334.
(47) Armstrong, F. A. *Struct. Bonding* **1990**, *72*, 137.
(48) Sagara, T.; Niwa, K.; Sone, A.; Hinnen, C.; Niki, K. *Langmuir* **1990**, *6*, 254.
(49) Davis, J. J.; Hill, H. A. O. *Chem. Commun.* **2002**, *5*, 393.
(50) Bizzarri, A. R.; Andolfi, L.; Stchakovsky, M.; Cannistraro, S. *J. Nanotechnol.* **2005**, *1*, 100.
(51) Wei, J.; Liu, H.; Dick, A. R.; Yamamoto, H.; He, Y.; Waldeck, D. H. *J. Am. Chem. Soc.* **2002**, *124*, 9591.
(52) Salamon, Z.; Hazzard, J. T.; Tollin, G. *Proc. Natl. Acad. Sci. U.S.A.* **1993**, *90*, 6420.
(53) Sagara, T.; Murumaki, H.; Igarashi, S.; Sato, H.; Niki, K. *Langmuir* **1991**, *7*, 3190.
(54) Cavalleri, O.; Natale, C.; Stroppolo, M. E.; Relini, A.; Cosulich, E.; Thea, S.; Novi, M.; Gliozzi, A. *Phys. Chem. Chem. Phys.* **2000**, *2*, 4630.
(55) Andolfi, L.; Cannistraro, S.; Canters, G. W.; Facci, P.; Ficca, A. G.; Van, Amsterdam, I. M. C.; Verbeet, M. Ph. *Arch. Biochem. Biophys.* **2002**, *399*, 81.
(56) Andolfi, L.; Bizzarri, A. R.; Cannistraro, S. *Thin Solid Films* **2006**, *515*, 212.
(57) Bonanni, B.; Bizzarri, A. R.; Cannistraro, S. *J. Phys. Chem. B* **2006**, *110*, 14574.
(58) The *N*-succinimidyl 3-maleimidopropionate (SMP) solution is prepared at 25 mM concentration in *N*,*N*-dimethylformamide (DMF). Full coverage of the Au(111) surface with maleimide groups is obtained by exposing the substrate to this solution for 40 min at room temperature.
(59) The *N*-succinimidyl-*S*-acetylthiopropionate (SATP) solution is prepared at 2 mM concentration in 10% dimethyl sulfoxide (DMSO) and 90% pH 7 phosphate-buffered saline (PBS) buffer. Room temperature incubation of the amino-terminated Au with this solution for 2 h provides full coverage of the Au surface with protected thiol groups. Deprotection is achieved by subsequent exposure of the modified substrate to a solution of 0.5 M hydroxylamine in pH 7 50 mM PBS, 25 mM ethylenediaminetetraacetic acid, and 50 mM dithiothreitol for 20 min. Samples were then rinsed with Milli-Q water (Millipore 18.2 MΩ).
(60) Ivarsson, A.; Hegg, P. O.; Lundstrom, I.; Jonsson, U. *J. Colloid Interface Sci.* **1985**, *13*, 169.
(61) Mrksich, M.; Sigal, G. B.; Whitesides, G. M. *Langmuir* **1995**, *11*, 4383.
(62) Kowalczyk, D.; Slomkowski, S. *J. Bioact. Compat. Polym.* **1994**, *9*, 282.
(63) Lu, J. R.; Su, T. J.; Thirtle, P. N.; Thomas, R. K.; Rennie, A. R.; Cubitt, R. J. *Colloid Interface Sci.* **1998**, *206*, 212.
(64) Binning, G; Rohrer, H; Gerber, C. *Phys. Rev. Lett.* **1982**, *49*, 57.
(65) Amrein, M. *STM and SFM in Biology*; Marti, O., Ed.; Academic Press Inc.: San Diego, CA, 1993.
(66) Binning, G.; Quate, C. F.; Gerber, C. *Phys. Rev. Lett.* **1986**, *56*, 930.
(67) Scheuring, S.; Ringler, P.; Borgnia, M.; Stahlberg, H.; Müller, D. J.; Agre, P.; Engel, A. *EMBO J.* **1999**, *18*, 4981.
(68) Zhong, Q.; Innis, D.; Kjoller, K.; Elings, V. B. *Surf. Sci.* **1993**, *290*, L688.
(69) Hoerber, J. K.; Miles, M. J. *Science* **2003**, *302*, 1002.
(70) Leatherman, G.; Durantini, E. N.; Gust, D.; Moore, T. A.; Moore, A. L.; Stone, S.; Zhou, Z.; Rez, P.; Liu, Y. Z.; Lindsay, S. M. *J. Phys. Chem. B* **1999**, *103*, 4006.
(71) Ishida, T.; Mizutani, W.; Aya, Y.; Ogiso, H.; Sasaki, S.; Tokumoto, H. *J. Phys. Chem. B* **2002**, *106*, 5886.
(72) Nahum, E.; Ebenstein, Y.; Aharoni, A.; Molari, T.; Banin, U.; Chimoni, N.; Millo, O. *Nano Lett.* **2004**, *4*, 103.
(73) Zhao, J.; Davis, J. J. *Nanotechnology* **2003**, *14*, 1023.
(74) Andolfi, L.; Cannistraro, S. *Surf. Sci.* **2005**, *598*, 68.
(75) Contera, S. A.; Iwasaki, H.; Suzuki, S. *Ultramicroscopy* **2003**, *97*, 65.
(76) (a) Zhang, J.; Christensen, H. E. M.; Ooi, B. L.; Ulstrup, J. *Langmuir* **2004**, *20*, 10200. (b) Hansen, A. G.; Boisen, A.; Nielsen, J. U.; Wackerbarth, H.; Chorkendor, I.; Andersen, J. E. T.; Zhang, J.; Ulstrup, J. *Langmuir* **2003**, *19*, 3419.
(77) (a) Zhang, J.; Chi, Q.; Kuznestov, A. M.; Hansen, A. G.; Wackerbarth, H.; Christensen, H. E. M.; Andersen, J. E. T.; Ulstrup, J. *J. Phys. Chem. B* **2002**, *106*, 1131. (b) Chi, Q.; Zhang, J.; Nielsen, J. U.; Friis, E. P.; Chorkendor, I.; Canters, G. W.; Andersen, J. E. T.; Ulstrup, J. *J. Am. Chem. Soc.* **2000**, *122*, 4047.
(78) Khomutov, G. B.; Belovolova, L. V.; Gubin, S. P.; Khanin, V. V.; Obydenov, A. Yu; Sergeev-Cherenkov, A. N.; Soldatov, E. S.; Trifonov, A. S. *Bioelectrochemistry* **2002**, *55*, 177.
(79) Xue, Y.; Datta, S.; Hong, S.; Reifenberger, R.; Henderson, J. I.; Kubiak, C. P. *Phys. Rev. B* **1999**, *59*, R7852.
(80) Bumm, L. A.; Arnold, J. J.; Dunbar, T. D.; Allara, D. L.; Weiss, P. S. *J. Phys. Chem. B* **1999**, *103*, 8122.
(81) Alliata, D.; Andolfi, L.; Cannistraro, S. *Ultramicroscopy* **2004**, *101*, 231.
(82) Campion, A.; Kambhampati, P. *Chem. Soc. Rev.* **1998**, *27*, 241.
(83) Moskovits, M. *Rev. Mod. Phys.* **1985**, *57*, 783.
(84) Stoecle, R. M.; Suh, Y. D.; Deckert, V.; Zenobi, R. *Chem. Phys. Lett.* **2000**, *318*, 131.
(85) Pettinger, B.; Picardi, G.; Schuster, R.; Ertl, G. *Single Mol.* **2002**, *5*, 285.
(86) Bizzarri, A. R.; Cannistraro, S. *J. Phys. Chem. B* **2005**, *109*, 16571.
(87) Rief, M.; Grubmüller, H. *ChemPhysChem* **2002**, *3*, 255.
(88) Hinterdorfer, P.; Baumgartner, W.; Gruber, H. J.; Schilcher, K.; Schindler, H. *Proc. Natl. Acad. Sci. U.S.A.* **1996**, *93*, 3477.
(89) Baumgartner, W.; Hinterdorfer, P.; Ness, W.; Raab, A.; Vestweber, D.; Schindler, H.; Drenckhahn. D. *Proc. Natl. Acad. Sci. U.S.A.* **2000**, *97*, 4005.
(90) Bell, G. I. *Science* **1978**, *200*, 618.
(91) Evans, E.; Ritchie, K. *Biophys. J.* **1997**, *72*, 1541.
(92) Dudko, O. K.; Filippov, A. E.; Klafter, J.; Urbakh, M.; *Poc. Natl. Acad. Sci. U.S.A.* **2003**, *100*, 11378.
(93) Kienberger, F.; Ebner, A.; Gruber, H. J.; Hinterdorfer, P. *Acc. Chem. Res.* **2006**, *39*, 29.
(94) Markiewicz, P.; Goh, M. C. *J. Vac. Sci. Technol., B* **1995**, *13*, 1115.
(95) Lukins, P. B.; Oates, T. *Biochim. Biophys. Acta* **1998**, *1409*, 1.
(96) Nar, H.; Messerschmidt, A.; Huber, R.; Van de Kamp, M.; Canters, G. W. *J. Mol. Biol.* **1991**, *218*, 427.
(97) Bizzarri, A. R.; Bonanni, B.; Costantini, G.; Cannistraro, S. *ChemPhysChem* **2003**, *4*, 1189.
(98) Delfino, I.; Bonanni, B.; Andolfi, L.; Baldacchini, C.; Bizzarri, A. R.; Cannistraro, S. *J. Phys: Condens. Matter* **2007**, submitted for publication.
(99) Tao, N. J. *Phys. Rev. Lett.* **1996**, *76*, 4066.
(100) Hildebrandt, P.; Stockburger, M. *J. Phys. Chem.* **1984**, *88*, 5935.
(101) Bizzarri, A. R.; Cannistraro, S. *Chem. Phys. Lett.* **2004**, *395*, 222.
(102) Persson, B. N. *Chem. Phys. Lett.* **1981**, *82*, 561.
(103) Schmickler, W.; Widrig, C. *J. Electroanal. Chem.* **1992**, *336*, 213.

(104) Lee, I.; Lee, J. W.; Greenbaum, E. *Phys. Rev. Lett.* **1997**, *79*, 3294.
(105) Komeda, T.; Kim, Y.; Kawai, M.; Persson, B. N. J.; Ueba, H. *Science* **2002**, *295*, 2055.
(106) Milani, M.; Andolfi, L.; Cannistraro, S.; Verbeet, M. Ph.; Bolognesi, M. *Acta Crystallogr., Sect. D* **2001**, *57*, 1735.
(107) Crowley, P. B.; Ubbink, M. *Acc. Chem. Res.* **2003**, *36*, 723.
(108) Florin, E.-L.; Moy, V. T.; Gaub, H. E. *Science* **1994**, *264*, 415.
(109) Zlatanova, J.; Lindsay, S. M.; Leuba, S. H. *Prog. Biophys. Mol. Biol.* **2000**, *74*, 37.
(110) Bonanni, B.; Kamruzzahan, A. S. M.; Bizzarri, A. R.; Rankl, C.; Gruber, H. J.; Hinterdorfer, P.; Cannistraro, S. *Biophys. J.* **2005**, *89*, 2783.
(111) Cutruzzola, F.; Arese, M.; Ranghino, G.; van Pouderoyen, G.; Canters, G.; Brunori. M. *J. Inorg. Biochem.* **2002**, *88*, 353.
(112) Bizzarri, A. R.; Brunori, E.; Bonanni, B.; Cannistraro, S. *J. Mol. Recognit.* **2007**, *20*, 1.
(113) For details on tip functionalization with the spacer and following C551 incubation, see ref 110.
(114) Kienberger, F.; Pastushenko, V. P.; Kada, G.; Gruber, H. J.; Riener, C.; Schindler, H.; Hinterdorfer, P. *Single Mol.* **2000**, *1*, 123.
(115) Ratto, T. V.; Langry, K. C.; Rudd, R. E.; Balhorn, R. L.; Allen, M. J.; McElfresh, M. W. *Biophys. J.* **2004**, *86*, 2430.
(116) Hinterdorfer, P.; Baumgartner, W.; Gruber, H. J.; Schilcher, K.; Schindler, H. *Proc. Natl. Acad. Sci. U.S.A.* **1996**, *93*, 3477.
(117) Wielert-Badt, S.; Hinterdorfer, P.; Gruber, H.; Lin, J. T.; Badt, D.; Wimmer, B.; Schindler, H.; Kinne, R. K.-H. *Biophys. J.* **2002**, *82*, 2767.
(118) Strunz, T.; Oroszlan, K.; Schumakovitch, I.; Güntherodt, H.-J.; Hegner, M. *Biophys. J.* **2000**, *79*, 1206.
(119) Yuan, C.; Chen, A.; Kolb, P.; Moy, V. T. *Biochemistry* **2000**, *39*, 10219.
(120) Schwesinger, F.; Ros, R.; Strunz, T.; Anselmetti, D.; Güntherodt, H.-J.; Honegger, A.; Jermutus, L.; Tiefenauer, L.; Pluckthun, A. *Proc. Natl. Acad. Sci. U.S.A.* **2000**, *97*, 9972.
(121) Fritz, J. A.; Katopodis, G.; Kolbinger, F.; Anselmetti, D. *Proc. Natl. Acad. Sci. U.S.A.* **1998**, *95*, 12283.
(122) Kokkoli, E.; Ochsenhirt, S. E.; Tirrell, M. *Langmuir* **2004**, *20*, 2397.
(123) Nooren, I. M. A.; Thornton, J. M. *J. Mol. Biol.* **2003**, *325*, 991.
(124) Dettmann, W.; Grandbois, M.; Andre', S.; Benoit, M.; Wehle, A. K.; Kaltner, H.; Gabius, H.-J.; Gaub, H. E. *Arch. Biochem. Biophys.* **2000**, *383*, 157.
(125) Willemsen, O. H.; Snel, M. M.; Cambi, A.; Greve, J.; De Grooth, B. G.; Figdor, C. G. *Biophys. J.* **2000**, *79*, 3267.
(126) Brogan, K. L.; Schoenfisch, M. H. *Langmuir* **2005**, *21*, 3054−3060.
(127) Sattin, B. D.; Pelling, A. E.; Goh, M. C. *Nucleic Acids Res.* **2004**, *32*, 4876.
(128) Basnar, B.; Elnathan, R.; Willner, I. *Anal. Chem.* **2006**, *78*, 3638.